

## Oscillatory channeled-ion scattering yield in beryllium

E. N. Kaufmann

*Bell Laboratories, Murray Hill, New Jersey 07974*

(Received 12 September 1977)

Strong oscillations in the Rutherford-backscattering yield of energetic  $^4\text{He}$  ions channeling in the basal plane of a beryllium single crystal have been observed. The wavelength of the oscillation is in reasonable agreement with a particle trajectory calculation using an analytical continuum potential, including the effects of thermal lattice vibrations, and is in good agreement with expectations from Monte Carlo simulations by Barrett.

### INTRODUCTION

Oscillations in the trajectories of ions undergoing planar channeling have been used in the past to study the validity of approximations to atomic potentials and stopping powers for channeled ions. We have observed pronounced oscillations in the Rutherford backscattering yield of channeled ions in beryllium metal. Since Be is a metal with only four electrons per atom, it may be asked whether the usual atomic potential approximations are valid in this case. We have compared our results with a continuum potential model as well as with Monte Carlo simulations and find reasonable agreement with both.

Using a Monte Carlo particle-channeling simulation program for a Au lattice, Barrett<sup>1</sup> has found that the parameter

$$q = \frac{1}{2} \lambda \psi_M / d_p \quad (1)$$

turns out to be extremely insensitive to the choice of atomic potential for scattering from the lattice atoms. In Eq. (1),  $\lambda$  is the wavelength of the oscillatory trajectories of particles which backscatter while undergoing planar channeling under conditions of perfect alignment of the ion beam with the channeling direction;  $\psi_M$  is a critical angle of incidence of the beam for which the maximum scattering yield is observed; and  $d_p$  is the interplanar lattice spacing. The insensitivity of  $q$  to details of the potential led Barrett to suggest that by measuring  $\psi_M$ , one could relate the measured value of  $\lambda$  in energy-loss units to the value of  $\lambda$  in depth units as extracted from Eq. (1), thereby obtaining an independent measure of the stopping power of the medium for the ions employed. Strong oscillations in yield of backscattered ions as a function of scattered-ion energy, while channeling in the basal plane (0001), were observed in the course of measurements on Be for the purpose of impurity lattice site determination.<sup>2</sup> Additional measurements were therefore made to evaluate the parameter  $q$  for comparison with Barrett's value for Au. This is the first such

measurement in beryllium. Previous studies of oscillatory planar channeling trajectories in other materials such as Fe,<sup>3</sup> Au,<sup>4</sup> Si,<sup>5</sup> and W,<sup>6</sup> have been reported.

### EXPERIMENTAL DETAILS

A Be single crystal, cut such that the normal to the sample lay in the (0001) plane midway between the  $\langle 11\bar{2}0 \rangle$  and  $\langle 10\bar{1}0 \rangle$  axes, was mounted on a  $25^\circ$  wedge in a two-axis goniometer and placed in the beam line of a 2-MV Van de Graaff accelerator. A  $^4\text{He}^+$  beam of 1.9-MeV energy, collimated to a beam divergence  $< 0.03^\circ$  was incident on the crystal and scattered ions were simultaneously detected in a 300-mm<sup>2</sup> annular Si surface-barrier detector centered at a scattering angle of  $180^\circ$  and in a solid detector placed at  $120^\circ$ . The  $120^\circ$  detector was masked to define the scattering angle to  $\pm 0.75^\circ$ , thus minimizing kinematic broadening in the energy spectrum (see Fig. 1).

The crystal was aligned using the relatively high count rate available in the  $180^\circ$  detector. When aligned for channeling in the (0001) plane, the crystal face was normal to the beam direction with the (0001) plane horizontal. Angular scans of the planar channel were performed by rotating the crystal about the normal to the goniometer holder (i.e., about an axis at  $25^\circ$  to the crystal normal). The accuracy with which the angle of incidence of the beam to the (0001) channel could be determined was  $\pm 0.004^\circ$ . The vertical acceptance angle of the masked  $120^\circ$  detector was sufficiently large to guarantee no influence of particle blocking (double alignment) on the data. Two advantages accrued from use of a  $120^\circ$  detector. First, the energy of He ions scattered at that angle from the surface of the sample was  $\sim 450$  keV whereas at  $180^\circ$  it is  $\sim 280$  keV which would have been more difficult to utilize in the presence of electronic noise and pulse pileup. And secondly, since scattered particles which have penetrated the crystal exit at  $120^\circ$  to the normal, their exit path lengths in the material are greater (by a factor of two) than they would have been in a  $180^\circ$

backscattering geometry, thus enhancing the overall depth resolution of the measurement. Figure 1 shows, in addition to a schematic diagram of the experimental geometry, a typical energy spectrum from the 120° detector as collected in a PDP-11/20 computer programmed as a multichannel analyzer.

The spectrum in Fig. 1 corresponds to perfect alignment of the incident beam with the (0001) channel. In addition to the events representing scattering from the matrix, peaks are observed at energies of ~668 and 881 keV due to scattering from thin surface layers of carbon and oxygen, respectively. The channel locations of these peaks were used in conjunction with the appropriate relation for kinematical energy loss at a 120° scattering angle<sup>7</sup> to determine the energy calibration of the spectra. Similar spectra were accumulated for equal integrated beam current at several angles of incidence  $\psi$  spanning values from perfect alignment with the (0001) plane to approximately twice the channeling critical angle.

## RESULTS AND DISCUSSION

The evolution of the large amplitude oscillatory behavior is clearly visible in the data of Fig. 1. From

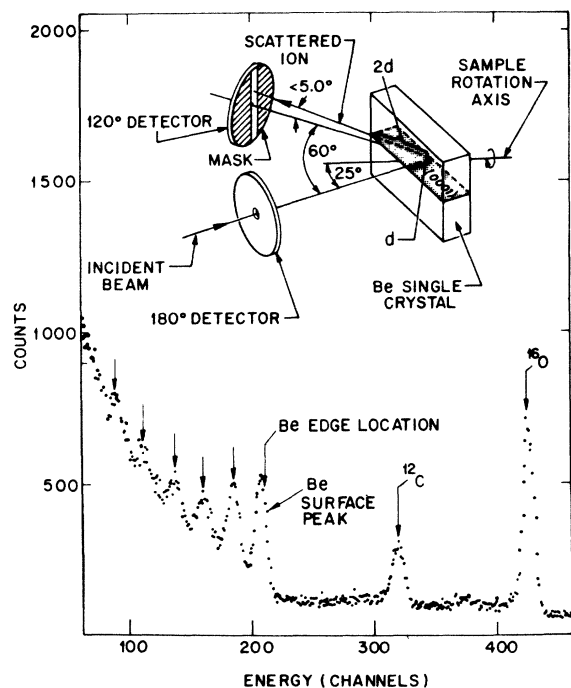


FIG. 1. Schematic diagram of experimental geometry and energy spectrum in 120° detector, for perfect alignment ( $\psi = 0$ ) with the (0001) channel. Yield oscillation maxima, the Be surface peak, and carbon and oxygen impurity peaks are shown. The flat background is primarily due to a bulk 20-ppm Ni impurity.

this spectrum, corresponding to  $\psi = 0$ , the energy position,  $E_M$ , of the first maximum below the surface peak was determined and used to compute a preliminary value for the half-wavelength  $\frac{1}{2}\lambda$  by using the relation

$$\frac{1}{2}\lambda = (kE_0 - E_M) / (kS_{in} + 2S_{out}) \quad (2)$$

where  $E_0$  is the incident beam energy,  $S_{in}$  and  $S_{out}$  are the stopping power values for He in Be corresponding to entrance and exit energies, respectively, and  $k$  is the kinematical scattering factor,<sup>7</sup>

$$k = \frac{M_1^2}{(M_1 + M_2)^2} \left\{ \cos\phi + \left[ \left( \frac{M_2}{M_1} \right)^2 - \sin^2\phi \right]^{1/2} \right\}^2 \quad (3)$$

which equals 0.2354 for  $M_1 = 4$ ,  $M_2 = 9$ , and  $\phi = 120^\circ$ . The stopping powers are rather slowly varying functions of ion energy. It is a reasonable approximation to neglect their variation over the entrance and exit paths due to energy loss. The large kinematic energy loss is accounted for by using appropriately different values for  $S_{in}$  and  $S_{out}$ . From the tables of Northcliffe and Schilling<sup>8</sup> for He in Be we find  $S_{in} = 270.7 \text{ keV}/\mu\text{m}$  for  $E_0 = 1.90 \text{ MeV}$  and  $S_{out} = 381.1 \text{ keV}/\mu\text{m}$  for  $E_{out} \approx 0.42 \text{ MeV}$ . Since tabulated energy-loss data refer to nonchanneled ions, a more precise value for  $S_{in}$  in our case would be somewhat greater<sup>9</sup> than quoted. However, since the first term in the denominator of Eq. (2) is less than 10% of the second term, we have neglected this correction. The resulting wavelength value was found to be  $\frac{1}{2}\lambda \approx 626 \pm 25 \text{ \AA}$ , where the error includes uncertainty in the position of the oscillatory maximum but does not include errors implicit in the tabulated stopping powers.

The energy loss of the beam in traversing thin impurity layers on the crystal surface would cause an essentially constant energy shift over the Be spectrum and would thus not affect our result. However, a polycrystalline layer of Be, in an oxide for example, would lead to an incorrect determination of the energy channel corresponding to the surface of the single crystal and in turn would lead to an overestimate of  $\frac{1}{2}\lambda$ . To correct for this possibility, we have used the area under the  $^{16}\text{O}$  peak in Fig. 1 along with the scattering yield from Be for a nonaligned incident beam to compute, employing the known relative Rutherford cross sections for He on  $^{16}\text{O}$  and  $^9\text{Be}$  in our geometry, the thickness of such an oxide layer assuming a composition of BeO. This resulted in a thickness of  $\sim 70 \text{ \AA}$  of oxide. With this value and stopping powers for BeO computed using Bragg's rule<sup>8</sup> we find the maximum correction to  $\frac{1}{2}\lambda$  is  $-88 \text{ \AA}$  yielding a corrected value of  $\frac{1}{2}\lambda = 538_{-25}^{+50} \text{ \AA}$ . The quoted error is increased asymmetrically on the high side, indicating the full correction of  $-88 \text{ \AA}$  is an overestimate since the effects of

(a) the lower density of Be in BeO as opposed to Be, (b) the greater stopping power of BeO over that of Be, and (c) the finite resolution of the detector would all tend to decrease the effect of the oxide layer on the experimentally determined location of the Be crystal edge in the spectra. The derived value of  $\frac{1}{2}\lambda$ , as corrected above, is in better agreement with the observed spacing of the deeper oscillatory maxima in Fig. 1 than is the uncorrected value.

For the evaluation of Eq. (1), the additional parameter  $\psi_M$  must be extracted from the data. The spectra for each angle  $\psi$  were smoothed using a three-point running average along the energy scale and are shown in Fig. 2. As the angle of incidence is varied, one sees from a careful examination of Fig. 2 that the first maximum below the surface moves closer to the surface peak. This indicates, as is expected, that the region of the first subsurface encounter of the particle trajectory with the host atom planes is moving to shallower depths. As the angle increases, the amplitude of this peak grows to a value which is the absolute yield maximum over the angle-depth plane. It is the angle  $\psi_M$  at which this maximum occurs that Barrett<sup>1</sup> has used in Eq. (1). In order to determine this angle more accurately, a portion of the data of Fig. 2, in-

cluding the region of the maximum, was displayed as a contour plot, as in Fig. 3. The maximum is inside the region indicated by the arrow and occurs at  $\psi_M = 0.254^\circ$  ( $4.43 \times 10^{-3}$  rad).

Introducing  $\psi_M$  (in radians),  $\frac{1}{2}\lambda$ , and  $d_p = 1.792 \text{ \AA}$  into Eq. (1), we find  $q_{\text{Be}} = 1.32^{+0.12}_{-0.06}$ . Barrett's<sup>1</sup> value for 1-MeV He in Au is  $q_{\text{Au}} = 1.36$ . Since one expects  $\psi_M \propto (E)^{-1/2}$  in analogy to a channeling critical angle and  $\lambda \propto (E)^{1/2}$  being proportional to ion velocity,  $q$  is independent of  $E$ . Therefore  $q_{\text{Au}}$  and  $q_{\text{Be}}$  may be directly compared and, within the quoted error, agreement is found. Monte Carlo simulations for the Be case would be desirable to determine whether  $q$  is indeed expected to be material independent.

To see whether the obtained value for  $\frac{1}{2}\lambda$  is in agreement with expectations on other grounds, we have computed the classical trajectory for a planar channeled He ion in Be using the continuum potential of Erginsoy<sup>10</sup> quoted by Barrett<sup>11</sup> which is based on a thermal average over a vibrating plane of atoms, each of which presents a scattering potential taken as Moliere's<sup>12</sup> approximation to a Thomas-Fermi function. Two parameters appearing in the potential which must be provided are the Thomas-Fermi screening length,  $a_{\text{TF}}$ , for He on Be and the root-mean-square thermal vibration amplitude,  $u_1$ , for Be at room temperature. The latter may be calculated in the Debye approximation, using  $^{13}\Theta_D = 1440 \text{ K}$  as the Debye temperature, to be  $u_1 = 0.06 \text{ \AA}$ . The expression for  $a_{\text{TF}}$  for the case of a completely ionized He ion interacting with Be is<sup>11</sup>

$$a_{\text{TF}} = 0.885 a_0 Z^{-1/3}, \quad (4)$$

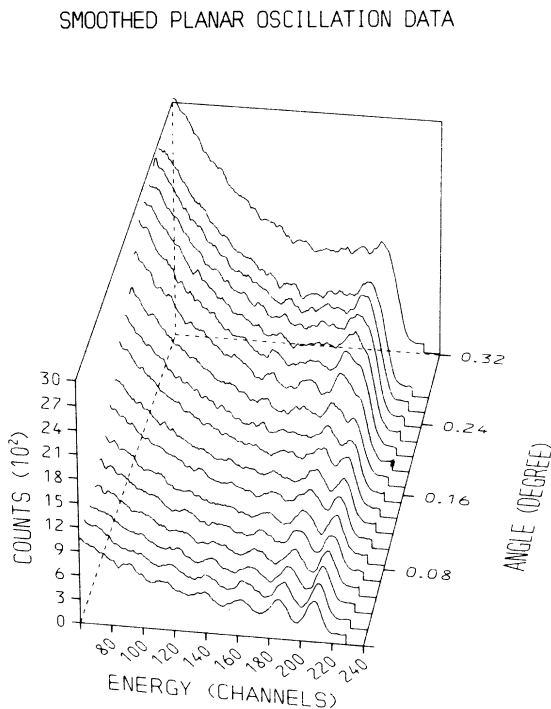


FIG. 2. Display of all smoothed energy spectra collected in the  $120^\circ$  detector as a function of angle of incidence. Note the movement of the first oscillatory maximum toward the surface as the angle of incidence increases.

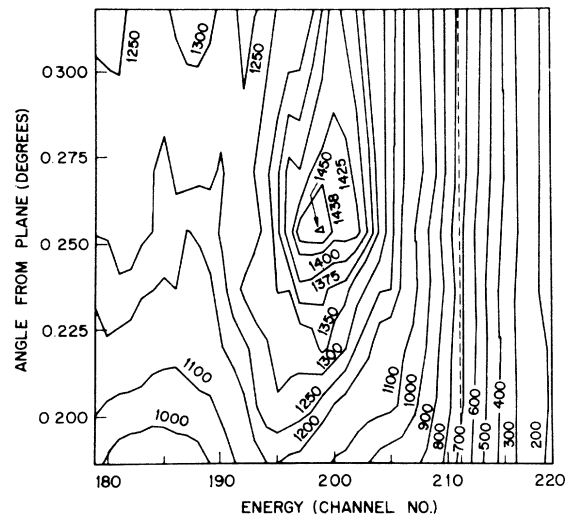


FIG. 3. Contour plot of smoothed data for the region of the angle-depth plane containing the absolute yield maximum. The dashed line corresponds to the position of the Be surface.

where  $a_0$  is the Bohr radius and the nuclear charge of Be is  $Z = 4$ . This yields  $a_{TF} = 0.295 \text{ \AA}$ , an unusually large value due to the low value of  $Z$ .

The potential, denoted  $V(X)$ , with the above parameter values, was used in two coupled differential equations for the position  $X$  and transverse velocity  $v$  of the particle,

$$v = \frac{dX}{dt}$$

and

$$-\frac{1}{m} \frac{d}{dX} [V(X) + V(d_p - X)] = \frac{dv}{dt} \quad (5)$$

where  $m$  is the He mass and  $t$  is time. From the initial conditions  $v(0) = 0$  and  $x(0) = b$ , the equations were numerically integrated stepwise in time until the next zero in transverse velocity was found. The time at which this zero occurred was translated into the penetration depth which corresponds to  $\frac{1}{2}\lambda$  using the known longitudinal velocity,  $(2E_0/m)^{1/2}$ . Since the oscillations in the experimental spectra are primarily due to particles entering the channel close to the walls,<sup>11</sup> the initial impact parameter value was taken as

$b \sim 0.05 \text{ \AA}$ . The result,  $\frac{1}{2}\lambda = 625 \text{ \AA}$ , is fortuitously close to the uncorrected experimentally derived value. Reasonable variations in the value of  $b$ , however, did not alter this result by more than  $25 \text{ \AA}$ .

Since thermal vibrations are included in the employed continuum model in a way which is known not to be rigorously correct,<sup>14</sup> the above obtained value is considered to be in reasonable agreement with experiment. This however reemphasizes the need for Monte Carlo simulation trials in Be which would properly account for lattice vibration while testing the sensitivity of the results to choice of potential. From the results presented here we can conclude that, even in a few-electron metal such as Be, the Thomas-Fermi potential is not an unreasonable approximation.

#### ACKNOWLEDGMENTS

The assistance of W. F. Flood, W. M. Augustyniak, M. F. Robbins, R. A. Boie, and J. W. Rodgers with various aspects of this work is gratefully acknowledged. Thanks for valuable discussions and advice are also extended to Dr. J. H. Barrett and Dr. J. A. Golovchenko.

<sup>1</sup>J. H. Barrett, Bull. Am. Phys. Soc. 21, 407 (1976); Annual Progress Report ORNL-5028 (UC-35-Physics), 1975, (unpublished), p. 23.  
<sup>2</sup>E. N. Kaufmann, P. Raghavan, R. S. Raghavan, E. J. Ansaldo, and R. A. Naumann, Phys. Rev. Lett. 34, 1558 (1975); E. N. Kaufmann, K. Krien, J. C. Soares, and K. Freitag, Hyperfine Interact. 1, 485 (1976); K. Krien, J. C. Soares, K. Freitag, R. Tischler, G. N. Rao, H. G. Müller, E. N. Kaufmann, A. Hanser, and B. Feuer, Phys. Rev. B 14, 4782 (1976); E. N. Kaufmann and R. Vianden, Phys. Rev. Lett. 38, 1290 (1977); E. N. Kaufmann, Phys. Lett. A 61, 479 (1977); K. Krien, H. Saitovich, K. Freitag, F. Reuschenbach, J. C. Soares, and E. N. Kaufmann, in Fourth International Conference on Hyperfine Interactions, Madison, N. J. June 13–17, 1977 (unpublished); B. Perscheid, H. W. Geyer, K. Krien, K. Freitag, J. C. Soares, E. N. Kaufmann, and R. Vianden, *ibid.*; R. Vianden and E. N. Kaufmann, in Third International Conference on Ion Beam Analysis, Washington, D. C., June 27–July 1, 1977 (unpublished).  
<sup>3</sup>F. Abel, G. Amsel, M. Bruneaux, C. Cohen and A. L'Hoir, Phys. Rev. B 12, 4617 (1975); and F. Abel, G. Amsel, M. Bruneaux and C. Cohen, Phys. Lett. A 42, 165 (1972).  
<sup>4</sup>J.-C. Poizat and J. Remillieux, J. Phys. (Paris) 33, 1013 (1972); M. J. Gailford, J. C. Poizat, and J. Remillieux, Phys. Lett. A 45, 325 (1973); S. Datz, C. D. Moak, T. S. Noggle, B. R. Appleton, and H. O. Lutz, Phys. Rev. 179,

315 (1969); S. Datz, C. D. Moak, B. R. Appleton, M. T. Robinson and O. S. Oen, in *Atomic Collision Phenomena in Solids*, edited by D. W. Palmer, M. W. Thompson, and P. D. Townsend (North-Holland, Amsterdam, 1970), p. 374; B. R. Appleton, S. Datz, C. D. Moak, and M. T. Robinson, Phys. Rev. B 4, 1452 (1971).  
<sup>5</sup>F. H. Eisen and M. T. Robinson, Phys. Rev. B 4, 1457 (1971).  
<sup>6</sup>E. Bøgh, Radiat. Eff. 12, 13 (1972).  
<sup>7</sup>J. B. Marion and F. C. Young, *Nuclear Reaction Analysis* (North-Holland, Amsterdam, 1968), p. 142.  
<sup>8</sup>L. C. Northcliffe and R. F. Schilling, Nucl. Data Tables A 7, Nos. 3–4 (1970).  
<sup>9</sup>Since particle groups contributing to oscillatory behavior have trajectories which lie close to atomic planes, they sample regions of above average electron density and would be expected to suffer greater than random electronic energy loss.  
<sup>10</sup>B. R. Appleton, C. Erginsoy, and W. M. Gibson, Phys. Rev. 161, 330 (1967).  
<sup>11</sup>J. H. Barrett, Phys. Rev. B 3, 1527 (1971).  
<sup>12</sup>G. Molière, Z. Naturforsch. A 2, 133 (1947).  
<sup>13</sup>*American Institute of Physics Handbook*, 3rd ed. (McGraw-Hill, New York, 1972), p. 4–115.  
<sup>14</sup>F. Abel, G. Amsel, M. Bruneaux, C. Cohen, and A. L'Hoir, Phys. Rev. B 13, 993 (1976).

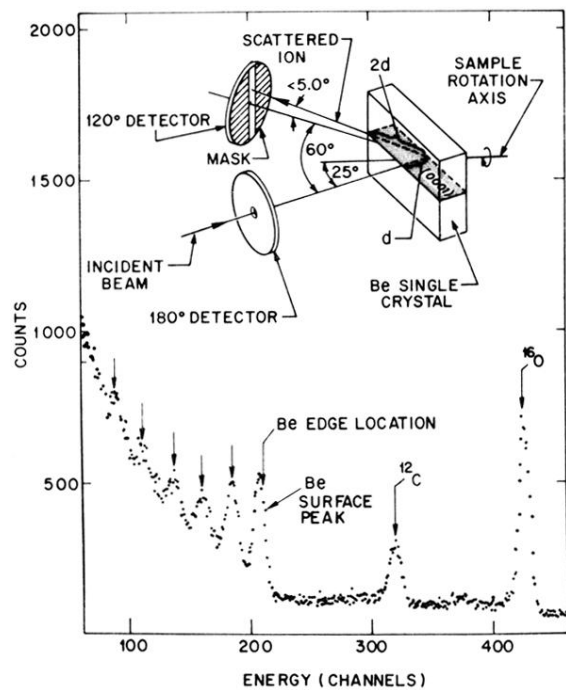


FIG. 1. Schematic diagram of experimental geometry and energy spectrum in  $120^\circ$  detector, for perfect alignment ( $\psi = 0$ ) with the (0001) channel. Yield oscillation maxima, the Be surface peak, and carbon and oxygen impurity peaks are shown. The flat background is primarily due to a bulk 20-ppm Ni impurity.